audioXPRESS
Tube, Solid State, Loudspeaker Technology

Article prepared for www.audioXpress.com

Horn Theory: An Introduction, Part 2

By Bjørn Kolbrek

The author continues his look at the various horn types and how they work.

SPHERICAL WAVE HORN

The spherical wave (or Kugelwellen) horn was invented by Klangfilm, the motion picture division of Siemens, in the late 1940s[26, 27]. It is often mistaken for being the same as the tractrix horn. It's not. But it is built on a similar assumption: that the wave-fronts are spherical with a constant radius. The wave-front area expansion is exponential.

To calculate the spherical wave horn contour, first decide a cutoff frequency f_c and a throat radius y_o (**Fig. 20**). The constant radius r_0 is given as

$$r_0 = \frac{c}{\pi f_c} \quad (18)$$

The height of the wave-front at the throat is

$$h_0 = r_0 - \sqrt{r_0^2 - y_0^2} \quad (19)$$

The area of the curved wave-front at the throat is

$$S_0 = 2\pi r_0 h_0$$

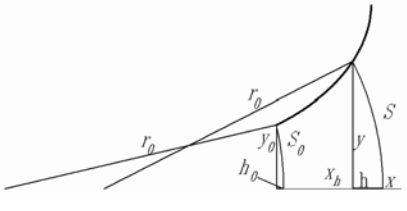

FIGURE 20: Dimensions of a spherical wave horn.

and the area of the wave-front with height h is $2\pi r_0 h$. Thus for the area to increase exponentially, h must increase exponentially:

$$h = h_0 e^{mx} \quad (20)$$

where x is the distance of the top of the wave-front from the top of the throat wave-front and

$$m = \frac{4\pi f_c}{c}.$$

Now that you know the area of the wave-front, you can find the radius and the distance of this radius from the origin.

$$S = 2\pi r_0 h$$

$$y = \sqrt{\frac{S}{\pi} - h^2} \quad (21)$$

$$x_h = x - h + h_0 \quad (22)$$

The assumed wave-fronts in a spherical wavehorn are shown in **Fig. 21**. Notice that the wave-fronts are not assumed to be 90° on the horn walls. Another property of the spherical wave horn is that it can fold back on itself (**Fig. 22**), unlike the tractrix horn, which is limited to a 90° tangent angle.

The throat impedance of a 100Hz spherical wave horn—assuming wave-fronts in the form of flattened spherical caps and using the radiation impedance of a sphere with radius equal to the mouth radius as mouth termination—is shown in **Fig. 23**. You can see that it is not very different from the throat impedance of a tractrix horn.

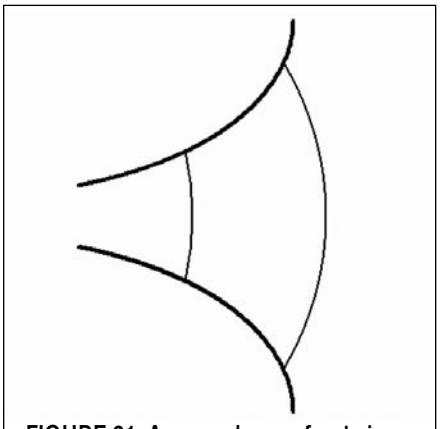

FIGURE 21: Assumed wave-fronts in spherical wave horns.

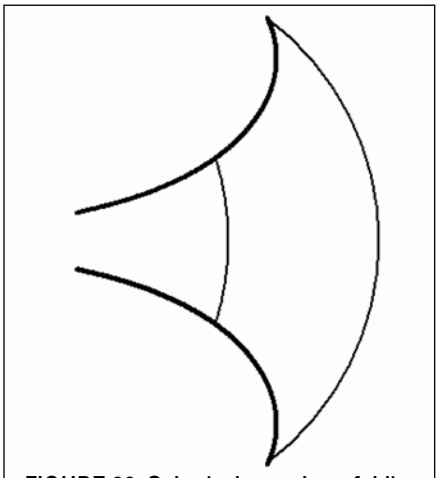

FIGURE 22: Spherical wave horn folding back.

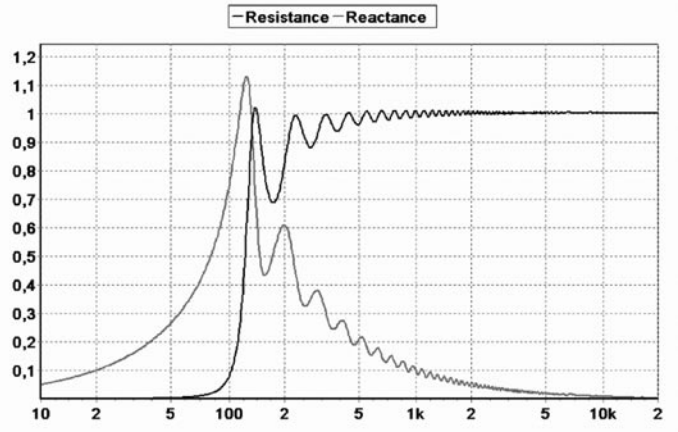

FIGURE 23: Throat impedance of a spherical wave horn.

LE CLÉAC'H HORN

Jean-Michel Le Cléac'h presented a horn that does not rely on an assumed wave-front shape. Rather, it follows a "natural expansion." The principle is shown in **Fig. 24**. Lines 0-1 show the wave-front surface at the throat (F1). At the point it reaches F2, the wave-front area has expanded, and to account for this, a small triangular element (or, really, a sector of a circle) b1 is added.

The wave-front expansion from b1 (line 3-4) continues in element a3, and an element b2 is added to account for further wave expansion at F3. The process is repeated, and the wave-front becomes a curved surface, perpendicular to the axis and the walls, but without making any assumptions regarding the shape prior to the calculations. The wave-fronts are equidistant from each other, and appear to take the shape of flattened spherical caps. The resulting contour of the horn is shown in **Fig. 25**.

The wave-front expands according to the Salmon family of hyperbolic horns. There is no simple expansion equation for the contour of the Le Cléac'h horn, but you can calculate it with the help of spreadsheets available at http://ndaviden.club.fr/pavillon/lecleah.html

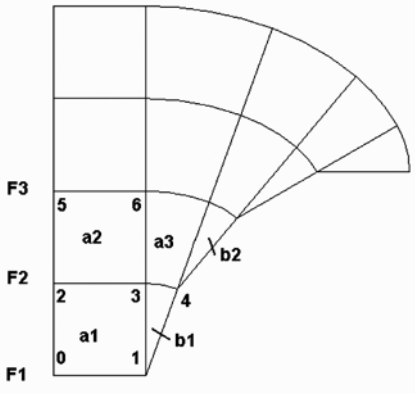

FIGURE 24: The principle of the Le Cléac'h expansion.

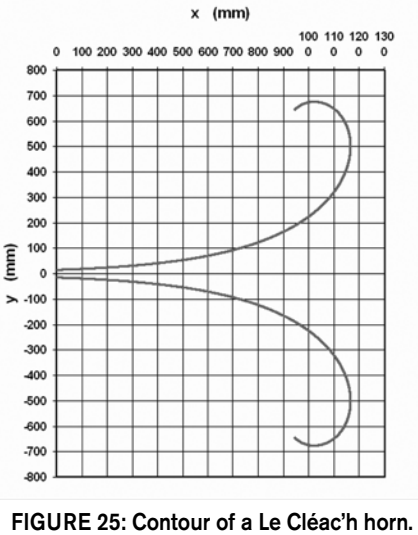

FIGURE 25: Contour of a Le Cléac'h horn.

OBLATE SPHEROIDAL WAVEGUIDE

This horn was first investigated by Freehafer[28], and later independently by Geddes[6], who wanted to develop a horn suitable for directivity control in which the sound field both inside and outside the horn could be accurately predicted. To do this, the horn needed to be a true 1P-horn. Geddes investigated several coordinate systems, and found the oblate spheroidal (OS) coordinate system to admit 1P waves. Putland[7] later showed that this was not strictly the case. More work by Geddes[29] showed that the oblate spheroidal waveguide acts like a 1P horn for a restricted frequency range. Above a certain frequency dictated by throat radius and horn angle, there will be higher order modes that invalidate the 1P assumptions.

The contour of the oblate spheroidal waveguide is shown in **Fig. 26**. It follows the coordinate surfaces in the coordinate system used, but in ordinary Cartesian coordinates, the radius of the horn as a function of x is given as

$$r = \sqrt{r_t^2 + \tan^2(\theta_0)x^2} \qquad (23)$$

where

r_t is the throat radius, and

θ_0 is half the coverage angle.

The throat acoustical impedance is not given as an analytical function; you must find it by numerical integration. The throat impedance for a waveguide with a throat diameter of 35.7mm and $\theta_0 = 30$ is shown in **Fig. 27**.

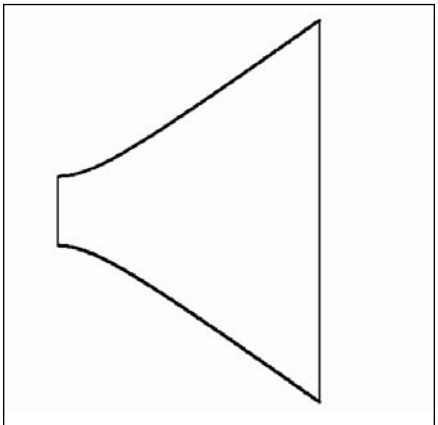

FIGURE 26: Contour of the oblate spheroidal waveguide.

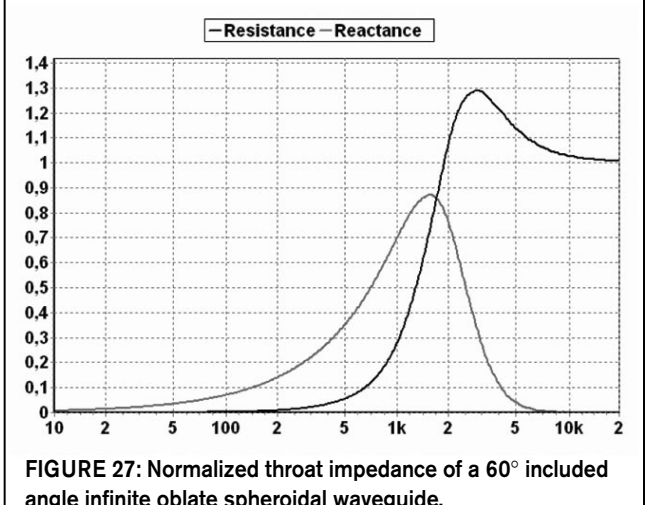

FIGURE 27: Normalized throat impedance of a 60° included angle infinite oblate spheroidal waveguide.

The OS waveguide does not have a sharp cutoff like the exponential or hyperbolic horns, but it is useful to be able to predict at what frequency the throat impedance of the waveguide becomes too low to be useful. If you set this frequency at the point where the throat resistance is 0.2 times its asymptotic value[30], so that the meaning of the cutoff frequency becomes similar to the meaning of the term as used with exponential horns, you get

$$f_c = \frac{0.2c}{\pi}\frac{\sin\theta_0}{r_t} \qquad (24)$$

You see that the cutoff of the waveguide depends on both the angle and the throat radius. For a low cutoff, a larger throat and/or a smaller angle is required. For example, for a 1″ driver and 60° included angle (θ_0 = 30), the cutoff is about 862Hz.

The advantages of the OS waveguide are that it offers improved loading over a conical horn of the same coverage angle, and has about the same directional properties. It also offers a very smooth transition from plane to spherical wave-fronts, which is a good thing, because most drivers produce plane wave-fronts.

The greatest disadvantage of the OS waveguide is that it is not suitable for low-frequency use. Bass and lower midrange horns based on this horn type will run into the same problems as conical horns: the horns become very long and narrow for good loading.

To sum up, the OS waveguide provides excellent directivity control and fairly good loading at frequencies above about 1kHz.

OTHER HORNS

Three other horn types assuming curved wave-fronts that are worth mentioning are: the Western Electric horns, the Wilson modified exponential, and the Iwata horn. What these horns have in common is that they do not assume curved wave-fronts of constant radius.

The Western Electric type horn[17] uses wave-fronts of constantly increasing radius, all being centered around a vertex a certain distance from the throat (**Fig. 29**).

In the Wilson modified exponential horn[31], the waves start out at the throat and become more and more spherical. The horn radius is corrected in an iterative process based on the wall tangent angle, and the contour lies inside that of the plane-wave exponential horn, being a little longer and with a slightly smaller mouth flare tangent angle (**Fig. 28**). Unfortunately, the Wilson method only corrects the wave-front areas, not the distance between the successive wave-fronts.

There is not much information available about the Iwata horn[32, 33], just a drawing and dimensions, but no description of the concept. It looks like a radial horn, and seems to have cylindrical wave-fronts expanding in area like a hypex-horn with T = √2. The ratio of height to width increases linearly from throat to mouth.

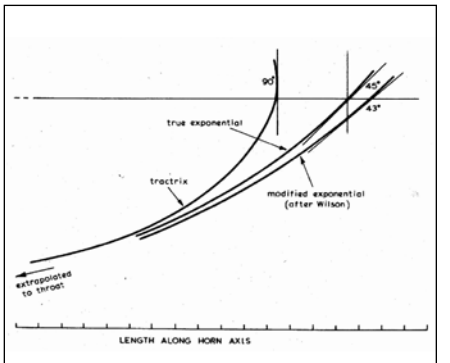

FIGURE 28: Comparison of the exponential horn with the tractrix and the Wilson modified exponential horn[22].

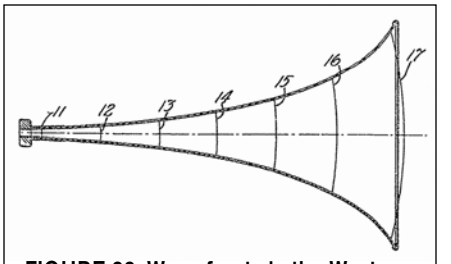

FIGURE 29: Wave-fronts in the Western Electric type exponential horn[17].

DIRECTIVITY CONTROL

Control of directivity is an important aspect of horn design. An exponential horn can provide the driver with uniform loading, but at high frequencies, it starts to beam. It will therefore have a coverage angle that decreases with frequency, which is undesirable in many circumstances. Often you want the horn to radiate into a defined area, spilling as little sound energy as possible in other areas. Many horn types have been designed to achieve this.

For the real picture of the directivity performance of a horn, you need the polar plot for a series of frequencies. But sometimes you also want an idea of how the coverage angle of the horn varies with frequency, or how much amplification a horn gives. This is the purpose of the directivity factor (Q) and the directivity index (DI)[34]:

Directivity Factor: The directivity factor is the ratio of the intensity on a given axis (usually the axis of maximum radiation) of the horn (or other radiator) to the intensity that would be produced at the same position by a point source radiating the same power as the horn.

Directivity Index: The directivity index is defined as: DI(f) = 10 $\log_{10}$ Q(f). It indicates the number of dB increase in SPL at the observation point when the horn is used compared to a point source.

Because intensity is watts per square meter, it is inversely proportional to area, and you can use a simple ratio of areas[35]. Consider a sound source radiating in all directions and observed at a distance r. At this distance, the sound will fill a sphere of radius r. Its area is $4\pi r^2$. The ratio of the area to the area covered by a perfect point source is 1, and thus Q = 1. If the sound source is radiating into a hemisphere, the coverage area is cut in half, but the same sound power is radiated, so the sound power per square meter is doubled. Thus Q = 2. If the hemisphere is cut in half, the area is 1/4 the area covered by a point source, and Q = 4.

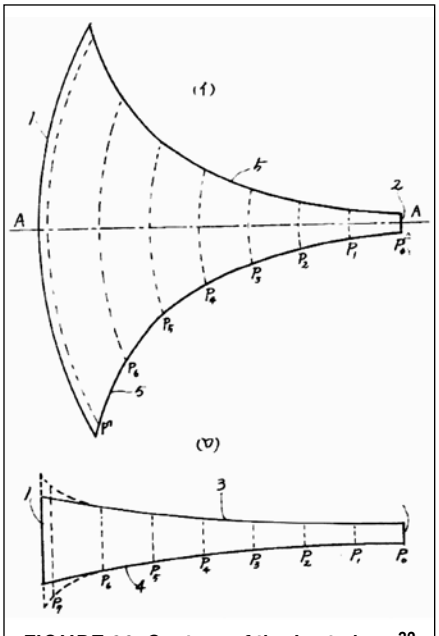

FIGURE 30: Contour of the Iwata horn[32].

For a horn with coverage angles α and β as shown in **Fig. 31**, you can compute Q as

$$Q = \frac{180}{\sin^{-1}\left(\sin\frac{\alpha}{2}\sin\frac{\beta}{2}\right)} \quad (25)$$

Most constant directivity horns try to act as a segment of a sphere. A sphere will emit sound uniformly in all directions, and a segment of a sphere will emit sound uniformly in the angle it defines, provided its dimensions are large compared to the wavelength[11]. But when the wavelength is comparable to the dimensions of the spherical segment, the beam width narrows to 40-50% of its initial value.

A spherical segment can control directivity down to a frequency given as

$$f_I = \frac{25 \cdot 10^6}{x \cdot \theta} \quad (26)$$

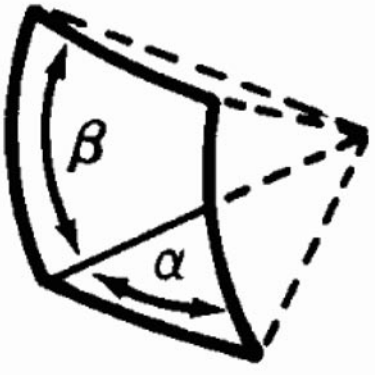

FIGURE 31: Radiation into a solid cone of space defined by angles α and β.

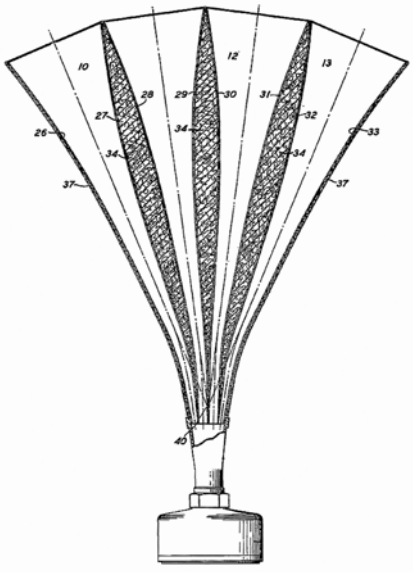

FIGURE 32: Multicellular horn[38].

where

f_I is the intercept frequency in Hz where the horn loses directivity control,

x is the size of the horn mouth in mm in the plane of coverage, and

θ is the desired coverage angle in degrees in that plane.

You thus need a large horn to control directivity down to low frequencies.

Most methods of directivity control rely on simulating a segment of a sphere. The following different methods are listed in historical order.

MULTICELLULAR HORNS

Dividing the horn into many conduits is an old idea. Both Hanna[36] and Slepian[37] have patented multicellular designs, with the conduits extending all the way back to the source. The source consists of either multiple drivers or one driver with multiple outlets, where each horn is driven from a separate point on the diaphragm.

The patent for the traditional multicellular horn belongs to Edward C. Wente[38]. It was born from the need to accurately control directivity, and at the same time provide the driver with proper loading, and was produced for use in the Bell Labs experiment of transmitting the sound of a symphonic orchestra from one concert hall to another[39].

A cut view of the multicellular horn, as patented by Wente, is shown in **Fig. 32**. In this first kind of multicellular horn, the individual horns started almost parallel at the throat, but later designs often used straight horn cells to simplify manufacture of these complex horns. As you can see, the multicellular horn is a cluster of smaller exponential horns, each with a mouth small enough to avoid beaming in a large frequency range, but together they form a sector of a sphere large enough to control directivity down to fairly low frequencies. The cluster acts as one big horn at low frequencies. At higher frequencies, the individual horns start to beam, but because they are distributed on an arc, coverage will still be quite uniform.

The multicellular horn has two problems, however. First, it has the same lower midrange narrowing as the ideal sphere segment, and, second, the polar pattern shows considerably "fingering" at high frequencies. This may not be as serious as has been thought, however. The -6dB beam widths of a typical multicellular horn are shown in **Fig. 33**. The fingering at high frequencies is shown in **Fig. 34**.

The beam width of a multicellular horn with different number of cells is shown in **Fig. 35**[34]. The narrowing in beam width where the dimensions of the horn are comparable to the wavelength is evident.

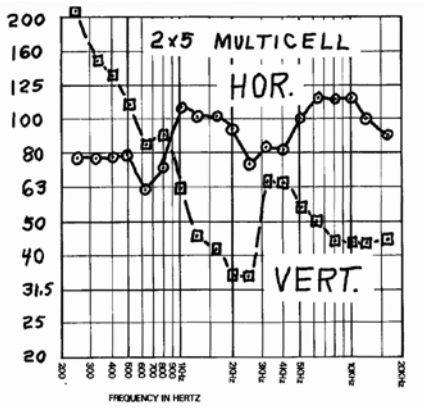

FIGURE 33: -6dB beam widths of Electro-Voice model M253 2 by 5 cell horn[42].

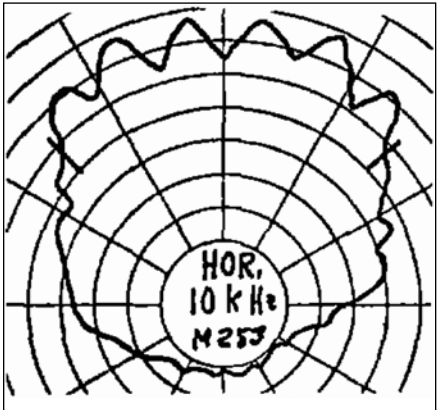

FIGURE 34: High frequency fingering of EV M253 horn at 10kHz[42].

RADIAL HORNS

The radial or sectoral horn is a much simpler concept than the multicellular horn. The horizontal and vertical views of a radial horn are shown in **Fig. 36**. The horizontal expansion is conical, and defines the horizontal coverage angle of the horn. The vertical expansion is designed to keep an exponential expansion of the wave-front, which is assumed to be curved in the horizontal plane. Directivity control in the horizontal plane is fairly good, but has the same midrange narrowing as the multicellular horn. In

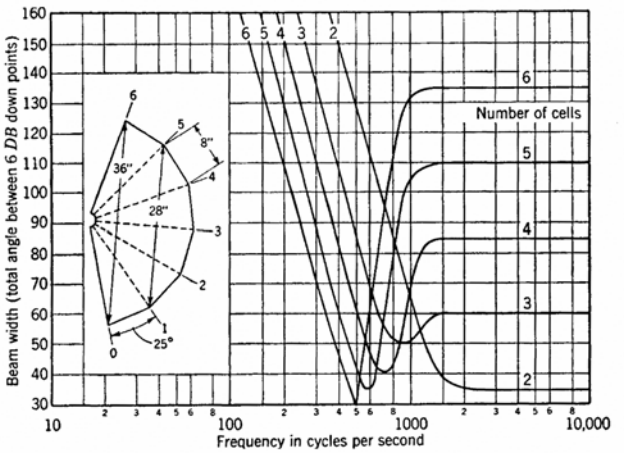

FIGURE 35: Beam width of a multicellular horn constructed as shown in the insert[34].

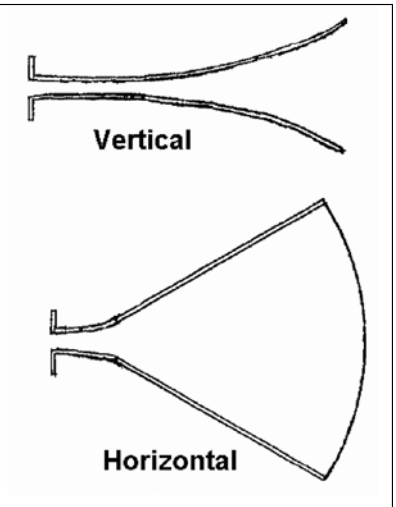

FIGURE 36: Profile of a radial horn[42].

addition, there is almost no directivity control in the vertical plane, and the beam width is constantly narrowing with increasing frequency.

REVERSED FLARE HORNS

The reversed flare horn can be considered to be a "soft diffraction horn," contrary to Manta-Ray horns and other modern constant directivity designs that rely on hard diffraction for directivity control. This class of horns was patented for directivity control by Sidney E. Levy and Abraham B. Cohen at University Loudspeakers in the early 1950s[40, 41]. The same geometry appeared in many Western Electric horns back in the early 1920s, but the purpose does not seem to be that of directivity control[17].

The principle for a horn with good horizontal dispersion is illustrated in **Fig. 37**. The wave is allowed to expand in the vertical direction only, then the direction of expansion is changed. The wave-front expansion is restricted vertically, and is released horizontally. The result is that the horizontal pressure that builds up in the first part of the horn causes the wave-front to expand more as it reaches the second part. That it is restricted in the vertical plane helps further.

Because the wave-front expansion is to be exponential all the way, the discontinuity at the flare reversal point (where the expansion changes direction) is small. In addition, the change of curvature at the flare reversal point is made smoother in practical horns than what is shown in the figure.

CE HORNS

In the early 1970s, Keele, then working for Electro-Voice, supplied an answer to the problems associated with multicellular and radial horns by introducing a completely new class of horns that provided both good loading for the driver and excellent directivity control[42].

The principle is based on joining an exponential or hyperbolic throat segment for driver loading with two conical mouth segments for directivity control. The exponential and conical segments are joined at a point where the conical horn of the chosen solid angle is an optimum termination for the exponential horn. Keele defines this as the point where the radius of the exponential horn is

$$r = \frac{0.95 \sin\theta}{k_c} \qquad (27)$$

where

r is the radius at the junction point,

θ is the half angle of the cone with solid angle Ω,

$$\theta = \cos^{-1}\left(1 - \frac{\Omega}{2\pi}\right), \text{ and}$$

k_c is the wave number at the cutoff frequency, $k_c = \frac{2\pi f_c}{c}$.

The problem of midrange narrowing was solved by having a more rapid flare close to the mouth of the conical part of the horn. Good results were obtained by doubling the included angle in the last third of the conical part. This decreases the acoustical source size in the frequency range of midrange narrowing, causing the beam width to widen, and removing the narrowing. The result is a horn with good directivity control down to the fre-

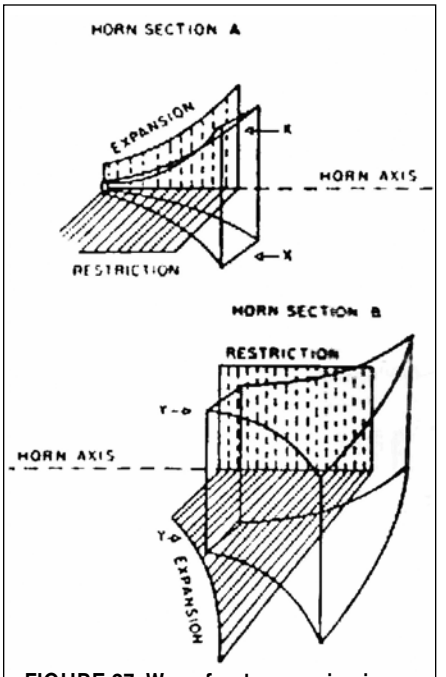

FIGURE 37: Wave-front expansion in reversed flare horns[41].

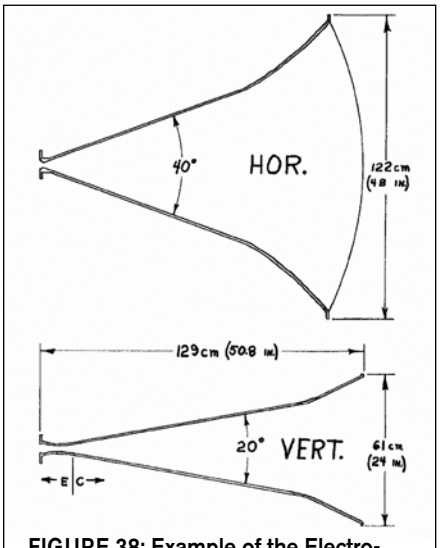

FIGURE 38: Example of the Electro-Voice CE constant directivity horns. This horn covers 40° by 20°[42].

quency dictated by the mouth size.

For a horn with different horizontal and vertical coverage angles, the width and height of the mouth will not be equal. The aspect ratio of the mouth will be given as

$$R = \frac{X_H}{X_V} = \frac{\sin\frac{\theta_H}{2}}{\sin\frac{\theta_H}{2}}, \quad (28)$$

or, if θ_H and θ_V are limited to 120°,

$$R \approx \frac{\theta_H}{\theta_V}. \quad (29)$$

The lower frequency of directivity control will also be dictated by the mouth aspect ratio. Substituting equation 26 into equation 29 and solving for the ratio of intercept frequencies, you get

$$\frac{f_{IH}}{f_{IV}} \approx \left(\frac{\theta_H}{\theta_V}\right)^2. \quad (30)$$

For a 40° by 20° (H-V) horn, the vertical intercept frequency will be four times higher than the horizontal intercept frequency.

MANTA-RAY HORNS

The Altec Manta-Ray horn sought to solve the problems of the CE horns, mainly the inability to independently specify the horizontal and vertical intercept frequencies[43]. To achieve directivity down to a lower frequency in the vertical plane, the vertical dimension of the mouth must be increased. Because the dispersion angle is smaller, the expansion must start further back, behind where the horizontal expansion starts. The result is the unique geometry shown in **Fig. 39** (although it's not so unique anymore).

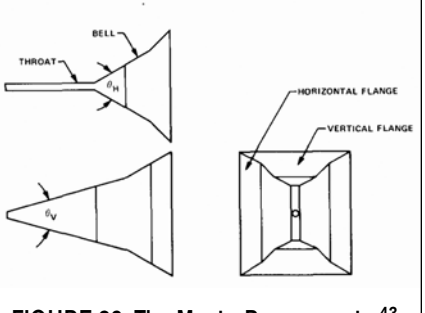

FIGURE 39: The Manta-Ray geometry[43].

At the point where the horizontal expansion starts, the wave is diffracted to fill the width of the horn, and dispersion is controlled by the horn walls.

The Manta-Ray horn incorporates the same rapid mouth flaring as the CE horns to avoid midrange narrowing, but does not use radial expansion of the walls. The reason for this is that radial walls produced a "waist-banding" effect, in which the horn lost much energy out to the sides in the upper midrange. This effect cannot be seen in the polar plots for the CE horns, which suggests that "waist-banding" can be a result of the Manta-Ray geometry, and not solely of radial wall contours.

NEW METHODS

Most newer constant directivity designs have been based on either the conical horn, some sort of radial horn (including the JBL Biradial design), or diffraction methods such as the Manta-Ray design. The only notable exception is the oblate spheroidal waveguide (covered previously) introduced by Geddes.

The general trend in horns designed for directivity control has been to focus on the control issue, because it is always possible to correct the frequency response. A flat frequency response does not, however, guarantee a perfect impulse response, especially not in the presence of reflections. Reflected waves in the horn at the high levels in question will also cause the resulting horn/driver combination to produce higher distortion than necessary, because the driver is presented with a nonlinear and resonant load. (See next section.)

DISTORTION

As mentioned, the horn equation is derived assuming that the pressure variations are infinitesimal. For the intensities appearing at the throat of horns, this assumption does not hold. Poisson showed in 1808 that, generally, sound waves cannot be propagated in air without change in form, resulting in the generation of distortion, such as harmonics and intermodulation products. The distortion is caused by the inherent nonlinearity of air.

If equal positive and negative increments of pressure are impressed on a mass of air, the changes in volume of that mass will not be equal. The volume change for positive pressure will be less than that for the equal negative pressure[44]. You can get an idea of the nature of the distortion from the adiabatic curve for air (**Fig. 40**). The undisturbed pressure and specific volume of air ($\frac{1}{\rho}$) is indicated in the point P_0V_0. Deviation from the tangent of the curve at this point will result in the generation of unwanted frequencies, the peak of the wave being stretched and the trough compressed.

The speed of sound is given as

$$c = \sqrt{\gamma\frac{p}{\rho}} \quad (31)$$

where

γ is the adiabatic constant of air, γ = 1.403.

You can see that the speed of sound increases with increasing pressure. So for the high pressure at the peaks of the wave-front, the speed of sound is higher than at the troughs. The result is that as the wave propagates, the peaks will gain on the troughs, altering the shape of the waveform and introducing harmonics (**Fig. 41**).

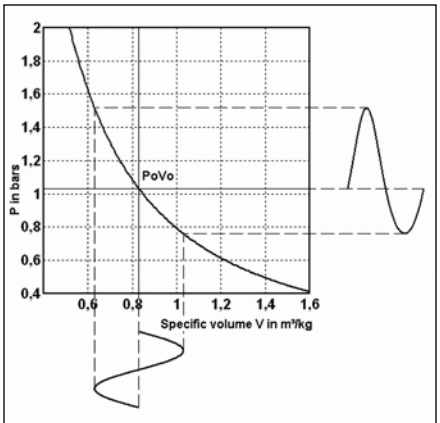

FIGURE 40: Adiabatic curve for air.

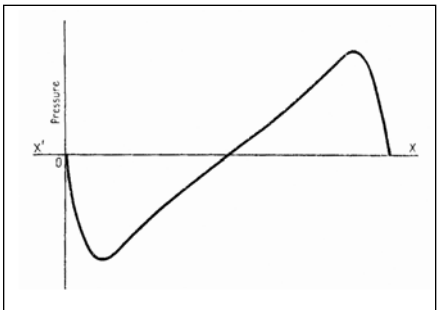

FIGURE 41: Distorted waveform due to non-constant velocity of sound[5].

There are thus two kinds of distortion of a sound wave: one because of the unequal alteration of volume, and another because of the propagation itself. This

last kind of distortion is most noticeable in a plane wave and in waves that expand slowly, as in horns, where distortion increases with the length propagated. Both kinds of distortion generate mainly a second harmonic component.

Fortunately, as the horn expands, the pressure is reduced, and the propagation distortion reaches an asymptotic value, which can be found for the horn in question, considering how it expands. It will be higher for a horn that expands slowly near the throat than for one that expands rapidly. For example, a hyperbolic-exponential horn with a low value for T will have higher distortion than a conical horn. For an exponential horn, the pressure ratio of second harmonic to fundamental is given as[44]

$$\frac{p_2}{p_1} = \frac{\gamma+1}{2\sqrt{2}} \frac{p_{1t}}{\gamma p_0} \frac{\omega}{c} \frac{-e^{-mx/2}}{m/2} \qquad (32)$$

where

p_{1t} is the RMS pressure of the fundamental at the throat,

p_1 is the RMS pressure of the fundamental at x,

p_2 is the RMS pressure of the second harmonic at x,

p_0 is the static pressure of air, and

m is the flare rate of the exponential horn.

You can see that distortion increases with frequency relative to the cutoff frequency. This is easier to see in the simplification for an infinite exponential horn given by Beranek[34]:

$$D_2[\%] = 1.73 \cdot 10^{-2} \frac{f}{f_c} \sqrt{I_t} \qquad (33)$$

where

I_t is the intensity at the throat, in watts per square meter.

Holland et al.[45] have investigated the distortion generated by horns both with the use of a computer model and by measurements. The model considered the harmonics required at the throat to generate a pure sine wave at the mouth (backward modeling), and also took reflections from the mouth into account. For a horn with a 400Hz cutoff and 4″throat, and a mouth SPL of 150dB, the distribution of harmonics is shown in **Fig. 42**. The peak at the cutoff frequency is due to the very high level required at the throat to generate the required SPL at the mouth.

Figure 43 shows the level of the harmonics at the throat at 1kHz for a given SPL at the mouth. Measurements showed that the prediction of the second harmonic level was quite accurate, but measured levels of the higher harmonics were higher than predicted. This was recognized as being due to nonlinearities in the driver.

As you can see from the results, the level of harmonics is quite low at the levels usually encountered in the home listening environment, but can be quite considerable in the case of high-level public address and sound reinforcement systems.

One point I need to mention is the importance of reducing the amount of reflection to reduce distortion. At the high levels involved, the reflected wave from diffraction slots or from the mouth will not combine with the forward propagating wave in a linear manner. The result will be higher distortion, and a nonlinear load for the driver. A driver working into a nonlinear load will not perform at its best, but will produce higher distortion levels than it would under optimum loading conditions[45].

Directivity of the horn also plays a role in the total distortion performance[46]. If the horn does not have constant directivity, the harmonics, because they are higher in frequency, will be concentrated toward the axis, while the fundamental spreads out more. This means that distortion will be higher on-axis than off-axis.

HIGHER ORDER MODES

At low frequencies, you can consider wave transmission in most horns as one-dimensional (1P waves). When the wavelength of sound becomes comparable to the dimensions of the horn, however, cross reflections can occur. The mode of propagation changes from the simple fundamental mode to what is called higher order modes. The behavior of these modes can be predicted for the uniform pipe and the conical horn[47, 48, 49], and it is found that they have cutoff frequencies below which they do not occur.

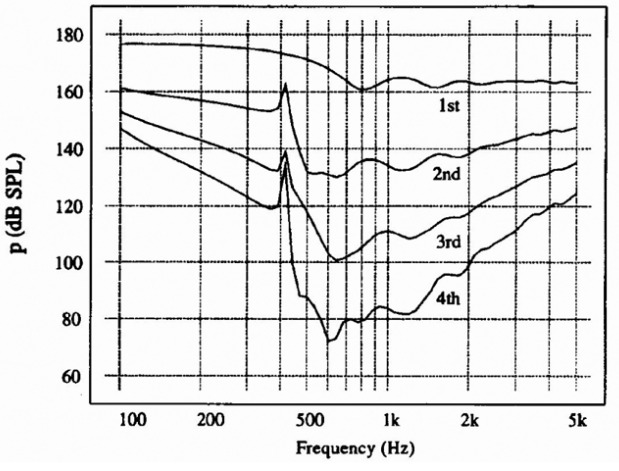

FIGURE 42: Level of harmonics at the throat for a sinusoidal mouth sound pressure level of 150dB, frequency sweep[45].

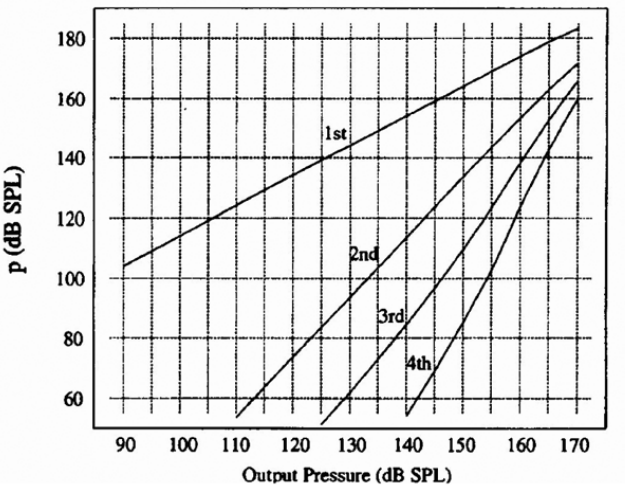

FIGURE 43: Level of harmonics at the throat for a 1kHz sinusoidal wave at the mouth, level sweep[45].

In 1925, Hoersch conducted a theoretical study of higher order modes in a conical horn, and calculated the equipressure contours for two kinds of modes. The results (**Fig. 44**) show the equipressure contours including both the radial and non-radial vibrations. The left part of the figure shows a pattern that resembles what Hall measured in a conical horn (Fig. 16). For a flaring horn such as the exponential, however, the higher order modes will occur at different frequencies at different places in the horn[8].

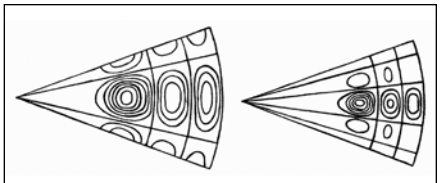

FIGURE 44: Higher order modes in a conical horn[47].

Higher order modes will also be generated by rapid changes in flare, such as discontinuities, so the slower and smoother the horn curvature changes, the less the chance for generating higher order modes.

The effect of the higher order modes is to disturb the shape of the pressure wave-front, so that directivity will be unpredictable in the range where the modes occur. According to Geddes, they may also have a substantial impact on the perceived sound quality of horns[50].

CLOSING REMARKS

In this article, I have tried to present both classical and modern horn theory in a comprehensive way. A short article like this can never cover all aspects of horns. But I hope it has provided useful information about how horns work, maybe also shedding light on some lesser known aspects and research.

Finally, I would like to thank Thomas Dunker and David McBean for proofreading, discussion, and suggestions.

aX

REFERENCES

26. Klangfilm GmbH., "Lautsprecher mit Exponentialtrichter," Swiss Patent no. 279947, 1948/1951.

27. H. Schmidt, "Über eine neuartige Lautsprecherkombination," Funk und Ton no. 5, 1950, pp. 226-232.

28. J.E. Freehafer, "The Acoustical Impedance of an Infinite Hyperbolic Horn," JASA vol. 11, April 1940, pp. 467-476.

29. E.R. Geddes, "Acoustic Waveguide Theory Revisited," *J*AES Vol. 41, No. 6, June 1993, pp.452-461.

30. D. Mapes-Riordan, "Horn Modeling with Conical and Cylindrical Transmission-Line Elements," *J*AES Vol. 41, No. 6, June 1993, pp. 471-484.

31. P. Wilson and G. Webb: "Modern Gramophones and Electrical Reproducers," Cassell and Company Ltd, 1929.

32. N. Iwata, Jap. patent no 54-59129, 1979.

33. J. Hiraga, *Les Haut-Parleurs*, 3rd edition, Dunod 2000.

34. L. Beranek, *Acoustics*, McGraw-Hill, 1954.

35. "Notes on Loudspeaker Directivity," Altec Technical Letter no. 211.

36. C.R. Hanna, "Multiple Inlet Horn," US Patent no. 1 715 706, 1925/1929.

37. J. Slepian, "Sound-Generating Device," US Patent no. 1 684 975, 1926/1928.

38. E.C. Wente, "Acoustic Device," US Patent no. 1 992 268, 1933/1935.

39. E.C. Wente and A.L. Thuras, "Loud Speakers and Microphones," BSTJ April 1934, pp. 259-277.

40. S.E. Levy and A.B. Cohen, "Acoustic Device," US Patent no. 2 690 231, 1950/1954.

41. A.B. Cohen, "Wide Angle Dispersion of High-Frequency Sound," *Audio Engineering*, Dec. 1952, pp. 24-25, 57-59.

42. D.B. Keele, "What's so Sacred About Exponential Horns?," AES preprint no. 1038, 1975.

43. C.A. Henricksen and M.S. Ureda, "The Manta-Ray Horns," *J*AES Vol. 26, No. 9, Sept. 1978, pp. 629-634.

44. A.L. Thuras, R.T. Jenkins, H.T. O'Neil, "Extraneous Frequencies Generated in Air Carrying Intense Sound Waves," BSTJ Jan. 1935, pp. 159-172.

45. K. Holland and C. L. Morfey, "A Model of Nonlinear Propagation in Horns," *J*AES Vol. 44, No. 7/8, Jul/Aug 1996, pp. 569-580.

46. T. Kikkawa, A. Yukiyoshi, and N. Sakamoto, "A New Horn Loudspeaker Design yields low Distortion and wide Dispersion," AES preprint no. 1151, 1976.

47. V.A. Hoersch, "Non-radial Vibrations Within a Conical Horn," Physical Review, Feb. 1925, pp. 218-224.

48. P.M. Morse and K.U. Ingard, "Theoretical Acoustics," 1968.

49. W.P. Mason, "Electromechanical Transducers and Wave Filters," Van Nostrand, 1942.

50. L.W. Lee and E.R. Geddes, "Audibility of Linear Distortion with Variations in Sound Pressure Level and Group Delay," AES ConventionPaper no. 6888, Oct. 2006.